DESY 17-040
MITP/17–016
March 2017

ISSN 0418–9833

Study of heavy meson production in p-Pb collisions at $\sqrt{S}$=5.02 TeV in the general-mass variable-flavour-number scheme

G. Kramer[1], and H. Spiesberger[2]

[1] II. Institut für Theoretische Physik, Universität Hamburg,
Luruper Chaussee 149, D-22761 Hamburg, Germany

[2] PRISMA Cluster of Excellence, Institut für Physik,
Johannes Gutenberg-Universität, 55099 Mainz, Germany,
and Centre for Theoretical and Mathematical Physics and Department of Physics,
University of Cape Town, Rondebosch 7700, South Africa

March 16, 2017

Abstract

We study inclusive charm and bottom production, for both D and B mesons, in p-Pb collisions at the LHC. Numerical results for p_T-differential production cross sections are obtained at next-to-leading-order in the general-mass variable-flavor-number scheme. We compare our results with recent data from ALICE and CMS at a center-of-mass energy of 5 TeV and find good agreement. A comparison with p-p cross sections does not reveal the presence of nuclear initial-state interaction effects that could be expected to become visible as deviations of the ratio of p-Pb and p-p cross sections from one.

PACS: 12.38.Bx, 12.39.St, 13.85.Ni, 14.40.Nd

1 Introduction

The study of heavy-quark (charm or bottom) production in p-p collisions at LHC energies is a useful test of perturbative Quantum Chromodynamics (QCD) since the heavy quark mass provides a hard scale that allows calculations within perturbation theory. The QCD calculations are based on the factorization approach, in which cross sections are calculated as a convolution of three terms: the parton distribution functions (PDF) of the incoming protons, the partonic hard scattering cross sections computed as a perturbative series in the strong interaction coupling constant, and the fragmentation functions (FF), describing the relative production yield and momentum distribution for a given heavy hadron (D or B meson) in a parton. Corresponding recent calculations at the perturbative level at next-to-leading order (NLO) with next-to-leading-log resummation (FONLL) [1, 2] or in the framework of the general-mass-variable-flavour-number scheme (GM-VFNS) [3, 4] have provided good descriptions for bottom meson production in $\bar{\text{p}}$-p collisions at $\sqrt{S} = 1.96$ TeV at the FNAL Tevatron Collider [5–7] and in p-p collisions at $\sqrt{S} = 7$ TeV at the CERN Large Hadron Collider (LHC) by the CMS, ATLAS and the LHCb collaborations [8–13]. The production cross section of charmed hadrons (D mesons) at the Tevatron [14] or of the ATLAS collaboration at the LHC [15] is also reasonably well described within theoretical and experimental uncertainties [16, 17].

The GM-VFNS is essentially the conventional NLO parton-model approach, supplemented with finite-mass effects, intended to improve the description at small transverse momentum p_T. The original GM-VFNS prescription [3, 4, 17] is, however, not suitable for calculations of the cross section $d\sigma/dp_T$ for heavy-quark hadron production at very small transverse momentum p_T. This is due to the specific choice of scale parameters for initial-state (μ_I) and final-state (μ_F) factorization. The original prescription was to set $\mu_I = \mu_F = \sqrt{m_Q^2 + p_T^2}$, where m_Q is the mass of the heavy quark, charm or bottom. At $p_T = 0$, the scale parameters approach $\mu_I = \mu_F = m_Q$, and at this point the heavy quark PDFs are put to zero by construction in almost all available PDF parametrizations. Therefore the transition to the fixed-flavour-number-scheme (FNNS), which is the appropriate scheme for calculating $d\sigma/dp_T$ at rather small p_T, is not reached for $p_T > 0$, since the heavy quark PDF in the proton decouples at $p_T = 0$, and not for finite $p_T > 0$.

A smooth transition to the FNNS at finite p_T can be achieved by exploiting the freedom to choose the factorization scale. In Refs. [18, 19] we have studied the prescription to fix the initial-state factorization scale at $\mu = 0.5\sqrt{m_Q^2 + p_T^2}$ instead of $\mu = \sqrt{m_Q^2 + p_T^2}$. For simplicity we have chosen the scales for initial and final state factorization equal to each other, $\mu_I = \mu_F$. With this scale choice we could achieve a reasonably good description of the data for B meson production down to $p_T = 0$ for the CDF data [6] in $\bar{\text{p}}$-p collisions at the Tevatron and of the LHCb data [13] for p-p collisions at the LHC in the forward rapidity region at $\sqrt{S} = 7$ TeV. A comparison of data for all D meson states D^0, D^+, D^{*+} and D_s^+ measured by the LHCb collaboration at $\sqrt{S} = 5$, 7 and 13 TeV with predictions from the GM-VFNS scheme with the original scale choice for $p_T > 3$ GeV can be found in [22–24].

The LHC Collaborations have also measured cross sections for heavy-quark production in p-Pb and Pb-Pb collisions. The ALICE collaboration, e.g., have performed detailed studies of the p_T-differential and rapidity-differential cross sections $d\sigma/dp_T$ and $d\sigma/dy$ for D-meson production in p-Pb collisions at $\sqrt{S} = 5.02$ TeV [25, 26], also for small p_T, as well as in Pb-Pb collisions at $\sqrt{S} = 2.76$ TeV [27]. Collisions with two heavy nuclei are of particular interest for studies of the Quark-Gluon Plasma (QGP), a high-density colour-deconfined medium. On the other hand, data from p-Pb collisions can be used to determine the nuclear modification factor $R_{\rm pPb}$, i.e., the ratio of p-Pb cross sections relative to the corresponding p-p cross sections scaled by the mass number of the Pb nucleus ($A = 208$). Data are in particular interesting at small p_T where one expects the largest deviation from $R_{\rm pPb} = 1$. The value of $R_{\rm pPb}$ is of interest for several reasons. First large deviations from one, in particular for larger p_T, would indicate the presence of initial-state interaction effects which are needed to obtain a reliable interpretation of corresponding Pb-Pb collision data. Second, the value of $R_{\rm pPb}$ is of interest by itself and could help to obtain information on the nuclear PDFs, which are modified compared to the proton PDFs in bound nucleons depending on the parton fractional momentum x and the atomic mass number A.

Ideally, measurements of the cross sections to determine the nuclear modification factor $R_{\rm pPb}$ should be done at the same center-of-mass energy $\sqrt{S}$. Unfortunately, this is not the case; data for p-p and p-Pb collisions at the same $\sqrt{S}$ are not available. Instead, the reference p-p cross section at $\sqrt{S} = 5.02$ TeV was obtained from data at $\sqrt{S} = 7$ TeV [28] by scaling the energy based on predictions from perturbative QCD. The scaling factor was determined for each D-meson species separately from the FONLL calculations [29]. In case of B meson production in p-Pb collisions at $\sqrt{S} = 5.02$ TeV, measured by the CMS collaboration [30], the reference cross section $d\sigma/dp_T$ for p-p collisions was directly taken from the FONNL calculations at $\sqrt{S} = 5.02$ TeV [29] without any extrapolation from their data at larger $\sqrt{S}$.

Due to the interest in the nuclear modification factor $R_{\rm pPb}$ for heavy quark hadron production, in particular as we expect to obtain important information about initial-state interaction effects in Pb-Pb collisions, it is desirable to study $R_{\rm pPb}$ also within other factorization schemes. This is the purpose of the present work in which we provide results from calculations of p-p cross sections $d\sigma/dp_T$ for D and B meson production at $\sqrt{S} = 5.02$ TeV in the framework of the GM-VFNS. We compare our results with data for the production of various D meson species at $\sqrt{S} = 5.02$ TeV measured by the ALICE collaboration [25, 26] and for B meson production at $\sqrt{S} = 5.02$ TeV measured by the CMS collaboration [30]. Using our results for the p_T-differential cross sections, we also study the nuclear modification factor $R_{\rm pPb}$.

The outline of our work is as follows. In the next section, Sect. 2, we give the details of the calculations for D mesons with the kinematic constraints of the ALICE experiment in the p_T range $1 < p_T < 24$ GeV. Section 3 contains our results for B meson production at $\sqrt{S} = 5.02$ TeV and a comparison with the CMS data. Section 4 is reserved for a discussion of the results.

2 D meson production in p-p and p-Pb collisions

The theoretical background and explicit analytic results of the GM-VFNS approach were previously presented in detail, see Refs. [3, 4] and the references cited therein. Here we only describe the input needed for the present numerical analysis.

Throughout this paper, we use the PDF set CTEQ14 [31] as implemented in the program library LHAPDF [32]. The fragmentation functions determined in Ref. [33] for D^0, D^+ and D^{*+} mesons and in Ref. [34] for the D_s^+ meson were used. These FFs always refer to the average over charge-conjugated states and our results below are understood as averaged cross sections $(\sigma(D) + \sigma(\overline{D}))/2$.

Originally, the default value for the scale parameters for renormalization and factorization were set by the transverse mass $m_T = \sqrt{m_Q^2 + p_T^2}$. By convention, variations around a default value by factors of two up and down were considered to obtain an estimate of unknown higher-order perturbative contributions and, thereby, assign a theoretical uncertainty to numerical results. We introduce the dimensionless parameters ξ_i $(i = R, I, F)$ and set $\mu_i = \xi_i m_T$. Independent variations of the ξ_i between 1/2 and 2 are restriced by keeping any ratio of the ξ_i's smaller than 2. We shall denote this choice of scales as the *original* prescription.

As already mentioned, this *original* scale choice does not provide a smooth transition to the FFNS at small p_T. To achieve this we change the factorization scales to $\mu_I = \mu_F = \xi_0\sqrt{4m_Q^2 + p_T^2}$ with $\xi_0 = 0.49$. A similar choice with $\xi_0 = 0.5$ was used in a recent study of charm meson production [20]. A forthcoming work, Ref. [21], using also $\xi_0 = 0.49$, found good agreement with data for p_T values down to $p_T = 0$. The choice of $\sqrt{4m_c^2 + p_T^2}$ in place of the transverse mass $m_T = \sqrt{m_c^2 + p_T^2}$ is motivated by the fact that the kinematic threshold for heavy-quark production is at $2m_c$ in the FFNS approach. With the additional factor $\xi_0 = 0.49$ we can ensure that $\mu = m_Q$ is reached already slightly above $p_T = 0$. For $m_Q = m_c = 1.3$ GeV one has $\mu = m_Q$ at $p_T = 0.528$ GeV. We choose this value of m_c to be consistent with the value used in the PDF set CTEQ14 from Ref. [31]; otherwise a smooth decoupling of the charm content of the proton PDF is not achieved. In our earlier calculations for larger values of p_T [17] we had adopted $m_c = 1.5$ GeV instead. We determine error bands for theoretical uncertainties from variations of the renormalization scale only, i.e., by varying ξ_R between 1/2 and 2. We have to leave the factorization scales unchanged since otherwise the proper transition to the FFNS would be lost. This setting of scales will be called the *modified* scale in the following.

With the *modified* scales a rather good agreement between theory predictions and LHCb data for the differential cross section $d\sigma/dp_T$ in various rapidity bins in the forward direction was observed in Ref. [21]. Before we apply this scale choice also for a comparison with the ALICE data in p-Pb collisions at small p_T [26], we have a look at the reference p-p cross section. The most precise data for the p_T-differential cross section of prompt D^0 meson production at $\sqrt{S} = 7$ TeV was obtained by a combination of measurements

without decay-vertex reconstructed in the low-p_T range, $0 < p_T < 2$ GeV, and an analysis using information from decay-vertex reconstruction at larger p_T, $2 < p_T < 16$ GeV. In all cases, the rapidity is restricted to the range $|y| < 0.5$ and contributions from the $b \to D^0$ transition have been subtracted. Data and results from the GM-VFNS are shown in Fig. 1 (left panel). The agreement with the default scale is very good in the large p_T range, $p_T > 6$ GeV, and for all p_T values the data points lie inside the theoretical range obtained from the scale variation of μ_R. The ratio of data for $d\sigma/dp_T$ normalized to our prediction in the GM-VFNS with the *modified* scale choice is shown in the right panel of Fig. 1. For the larger $p_T \geq 6$ GeV the ratio is equal to one within the experimental accuracy. This is consistent with the prediction of the *original* scale choice, for which the same ratio was shown in Ref. [26] for $p_T \geq 3$ GeV. For the smaller p_T, $1 < p_T < 6$ GeV, the ratio in Fig. 1 (right panel) increases to approximately 1.5. This is very similar to results based on the FONLL approach [29] and on the LO k_T factorization calculation [35], which was

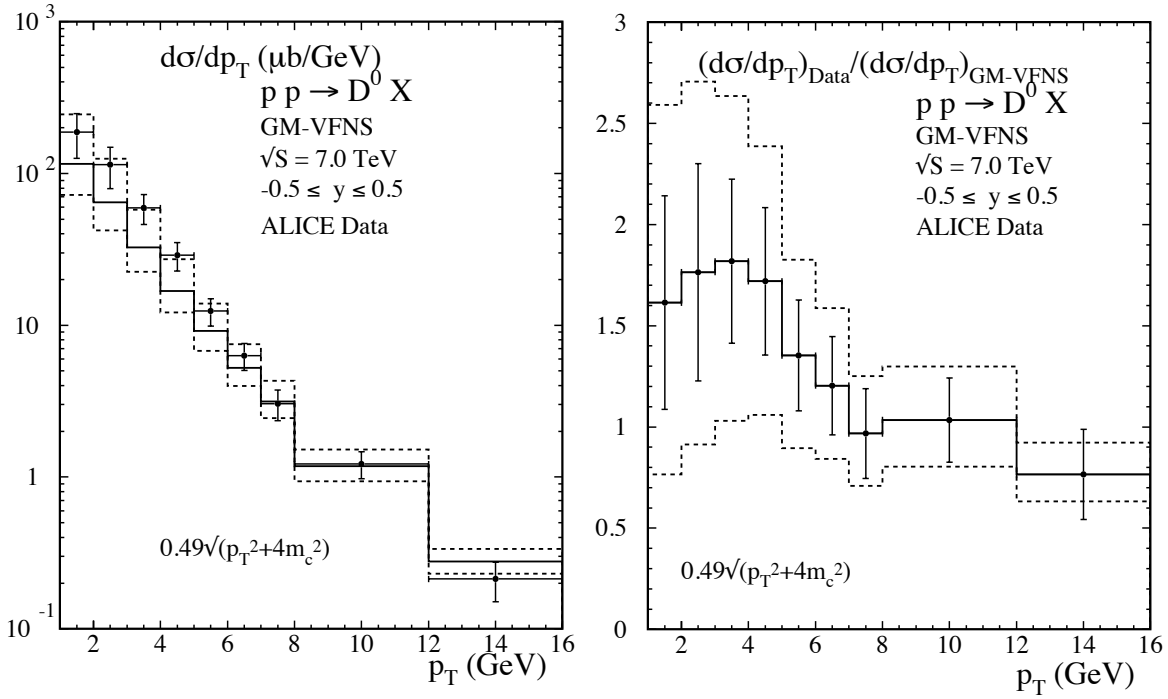

Figure 1: Left panel: Differential production cross section $d\sigma/dp_T$ of prompt D^0 mesons in p-p collisions at $\sqrt{S} = 7$ TeV with $|y| < 0.5$ in the p_T interval $1 < p_T < 16$ GeV compared to ALICE data [26, 28]. The data point for the bin $1 < p_T < 2$ GeV is from the analysis [26], while the data points for $2 < p_T < 16$ GeV are taken from [28]. The theoretical cross sections are calculated in the GM-VFNS with default scales $\mu_R = \sqrt{4m_c^2 + p_T^2}$ and $\mu_I = \mu_F = 0.49\sqrt{4m_c^2 + p_T^2}$. The upper and lower dashed histograms are calculated with μ_R changed by factors 1/2 and 2. Right panel: Ratios of the ALICE data over theory predictions.

also shown in [26]. We remark that inside the scale variation (see the dashed lines in Fig. 1, right panel) the ratio of data over GM-VFNS predictions is compatible with one.

Now we continue with a comparison of theory predictions and ALICE data for p-Pb collisions. Theoretical predictions are obtained from the p-p cross section by multiplication with the mass number $A = 208$, $Ad\sigma/dp_T$. Data are available at $\sqrt{S} = 5.02$ TeV in the rapidity region $|y| < 0.5$. Our results in the GM-VFNS with the *modified* scale choice are shown in Figs. 2, 3, 4, and 5 (left panels) for D^0, D^+, D^{*+} and D_s^+ production, in each case together with the data from [26] as a function of p_T for bins in the range $1 < p_T < 24$ GeV. Except for two points at the largest p_T (see Figs. 3 and 4) the error bars of the data points overlap with the uncertainty range due to scale variations. As for p-p collisions, the ALICE data shown in Fig. 2 are obtained for prompt D^0 production in the interval $0 < p_T < 2$ GeV (only data for $p_T > 1$ GeV are shown) without decay-vertex reconstruction [26] and for $p_T > 2$ GeV with decay-vertex reconstruction [25]. The data for the other three D-meson species D^+, D^{*+} and D_s^+ are taken from Ref. [25].

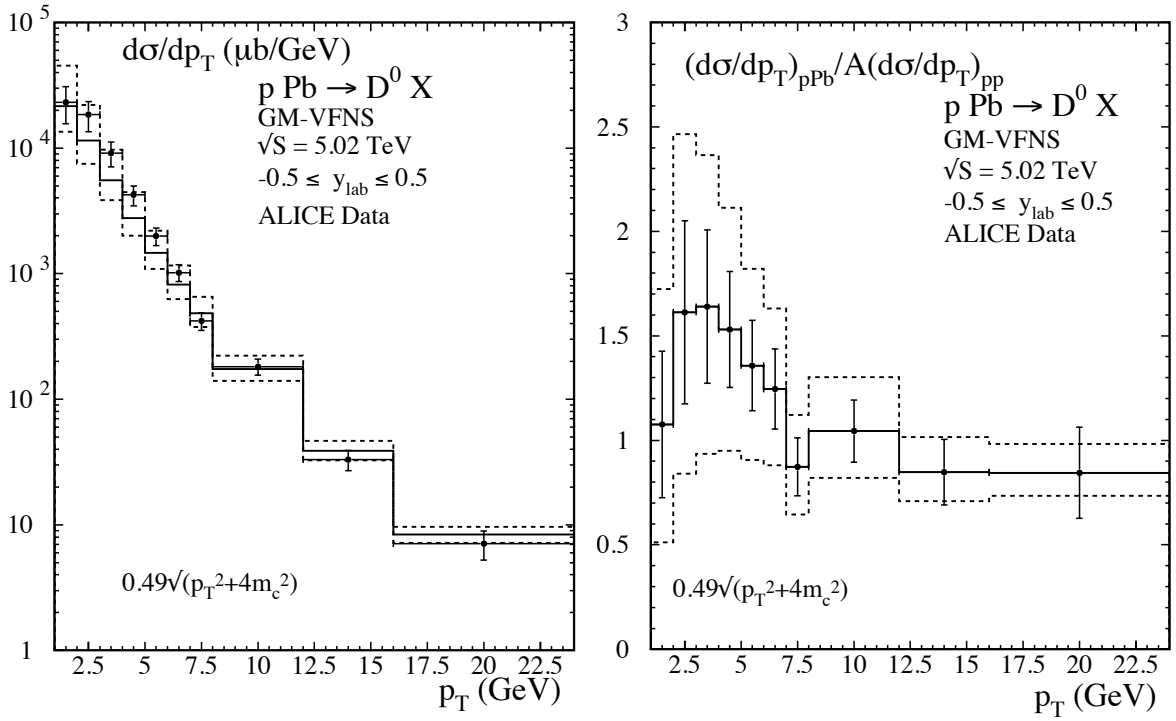

Figure 2: Left panel: Differential production cross section $d\sigma/dp_T$ of prompt D^0 mesons in p-Pb collisions at $\sqrt{S} = 5.02$ TeV with $|y| < 0.5$ of ALICE data [26] compared to A times the respective p-p reference cross section calculated in the GM-VFNS with default scales $\mu_R = \sqrt{4m_c^2 + p_T^2}$ and $\mu_I = \mu_F = 0.49\sqrt{4m_c^2 + p_T^2}$. The upper and lower dashed histograms are calculated with μ_R changed by factors 1/2 and 2. Right panel: Ratios of the ALICE data over theory predictions.

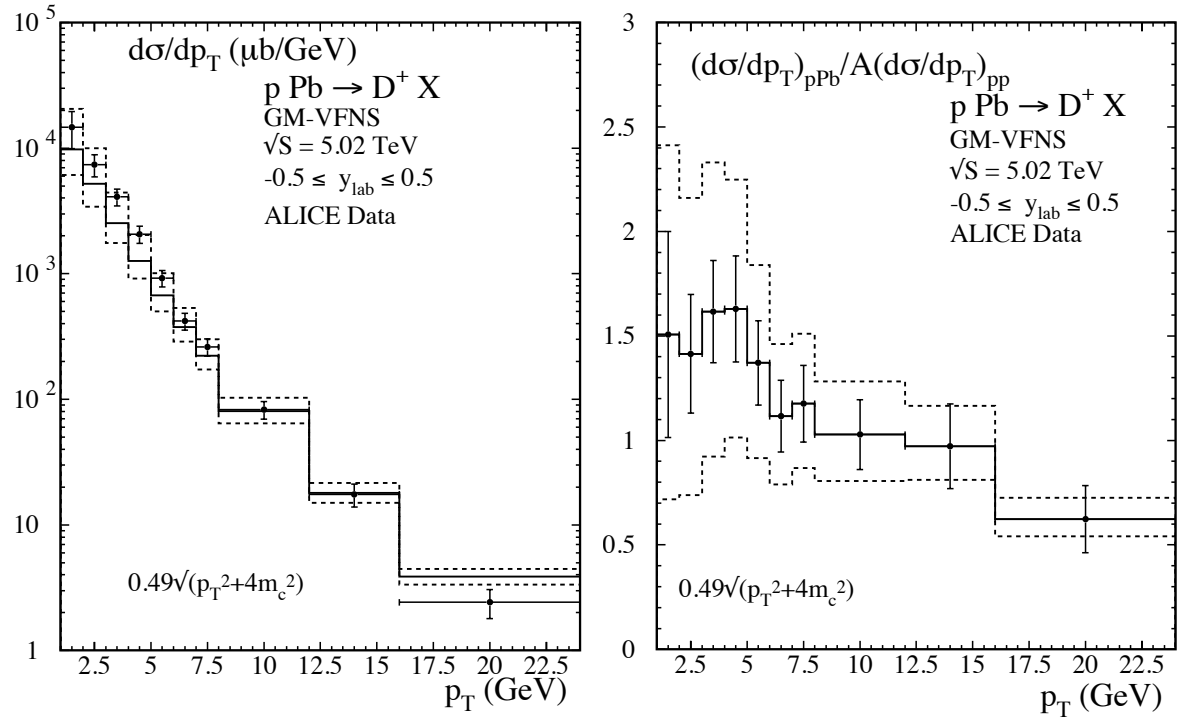

Figure 3: Left panel: Differential production cross section $d\sigma/dp_T$ of prompt D^+ mesons in p-Pb collisions at $\sqrt{S} = 5.02$ TeV with $|y| < 0.5$ of ALICE data [26] compared to A times the respective p-p reference cross section calculated in the GM-VFNS with default scales $\mu_R = \sqrt{4m_c^2 + p_T^2}$ and $\mu_I = \mu_F = 0.49\sqrt{4m_c^2 + p_T^2}$. The upper and lower dashed histograms are calculated with μ_R changed by factors 1/2 and 2. Right panel: Ratios of the ALICE data over theory predictions.

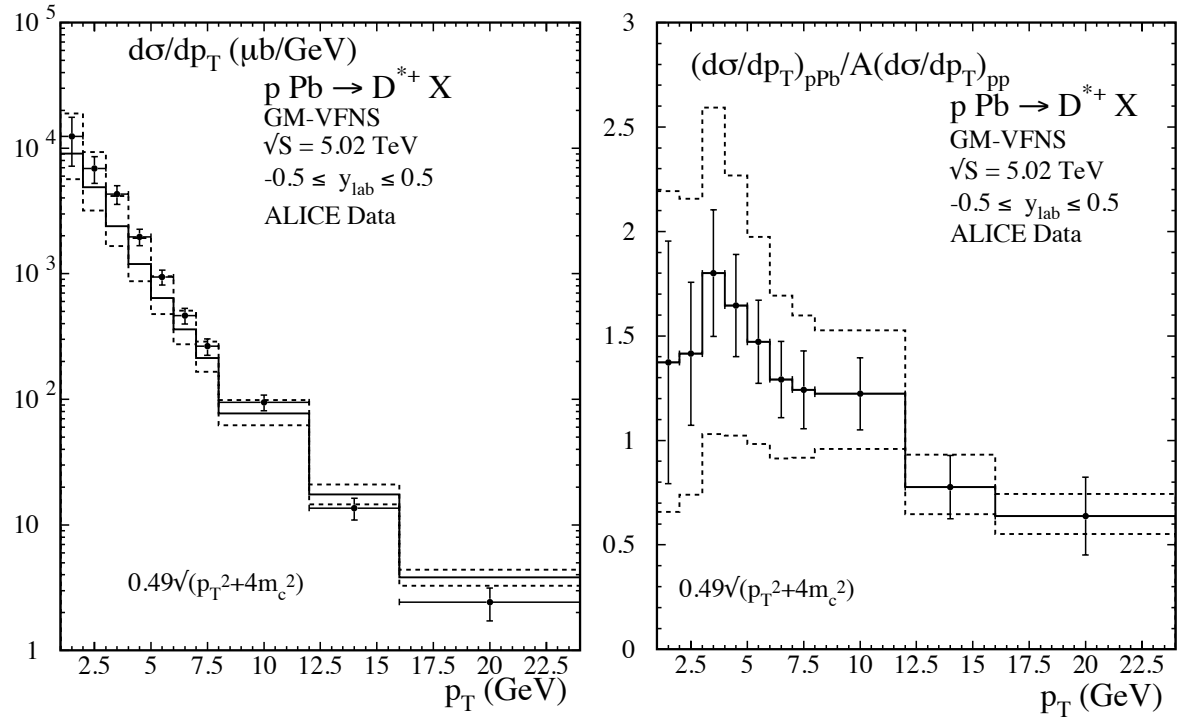

Figure 4: Left panel: Differential production cross section $d\sigma/dp_T$ of prompt D^{*+} mesons in p-Pb collisions at $\sqrt{S} = 5.02$ TeV with $|y| < 0.5$ of ALICE data [26] compared to A times the respective p-p reference cross section calculated in the GM-VFNS with default scales $\mu_R = \sqrt{4m_c^2 + p_T^2}$ and $\mu_I = \mu_F = 0.49\sqrt{4m_c^2 + p_T^2}$. The upper and lower dashed histograms are calculated with μ_R changed by factors 1/2 and 2. Right panel: Ratios of the ALICE data over theory predictions.

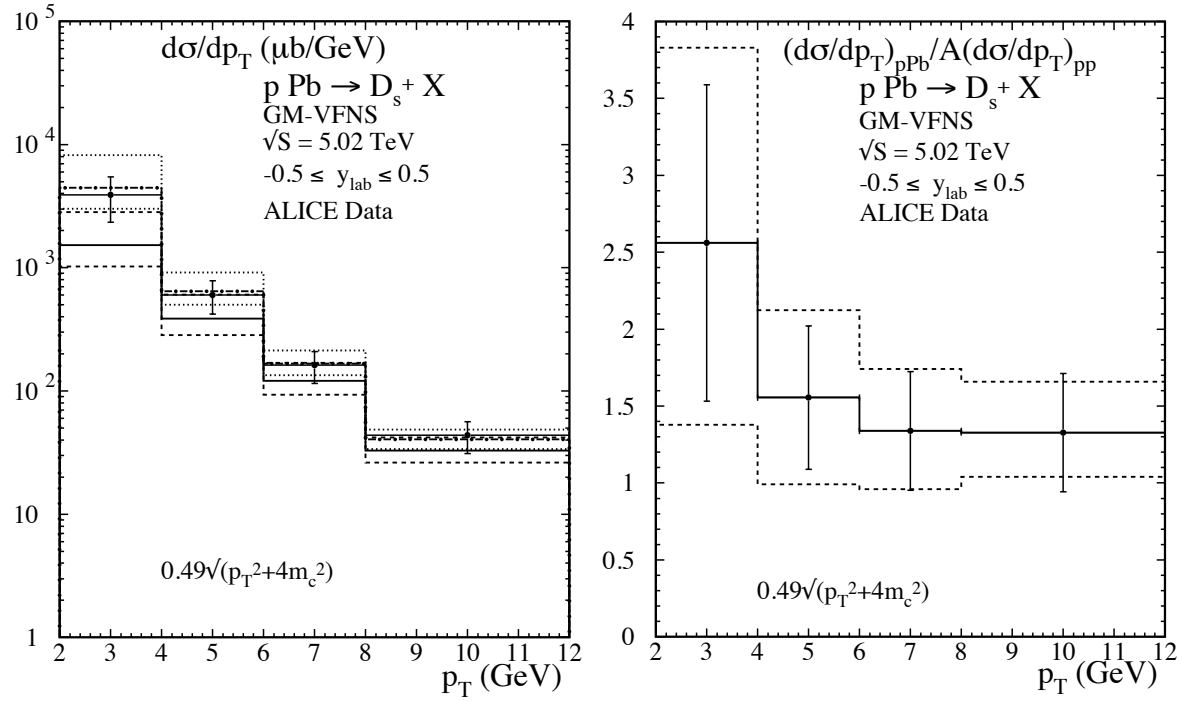

Figure 5: Left panel: Differential production cross section $d\sigma/dp_T$ of prompt D_s^+ mesons in p-Pb collisions at $\sqrt{S} = 5.02$ TeV with $|y| < 0.5$ of ALICE data [26] compared to A times the respective p-p reference cross section calculated in the GM-VFNS with default scales $\mu_R = \sqrt{4m_c^2 + p_T^2}$ and $\mu_I = \mu_F = 0.49\sqrt{4m_c^2 + p_T^2}$. The upper and lower dashed histograms are calculated with μ_R changed by factors 1/2 and 2. The dashed-dotted histogram is obtained for the *original* scale choice and the light dotted histograms for its corresponding scale variations. Right panel: Ratios of the ALICE data over theory predictions for the *modified* scale choice.

Corresponding ratios for ALICE data normalized to our theoretical results for $Ad\sigma/dp_T$ are presented in the right panels of Figs. 2, 3, 4, and 5. The ratio for D^0 production (Fig. 2) looks rather similar to the ratio at $\sqrt{S} = 7$ TeV for p-p collisions (Fig. 1). The similarity between p-p and p-Pb collisions is even more clearly visible when we consider the ratio of the results shown in the right panels of Figs. 1 and 2. This is done in Fig. 6. The error bars shown here represent the uncertainty of the p-Pb data only, but this is sufficient to conclude that, with the present errors on the data, it is difficult to claim the presence of an additional deviation of the ratio from one caused by corrections due to initial-state interactions in the Pb nucleus.

For the other mesons, D^+, D^{*+} and D_s^+ in Figs. 3, 4, and 5 the pattern of ratios looks also quite similar. For the larger p_T bins the ratio is equal to one within errors, and for the smaller p_T bins the ratio is close to 1.5. We remark that the nuclear modification factor $R_{\rm pPb}$ is consistent with one for all four D meson species if the theoretical uncertainty due to scale variations is taken into account except maybe for the first p_T bin in Fig. 5 (right panel) for D_s^+ production.

We can compare our results with the nuclear modification factor presented in Ref. [26]. The ratios $R_{\rm pPb}$ for D^0, D^+ and D^{*+} given there are much closer to one than our calculated ratios shown in Figs. 2, 3, and 4. One can speculate that this is due to the fact that in

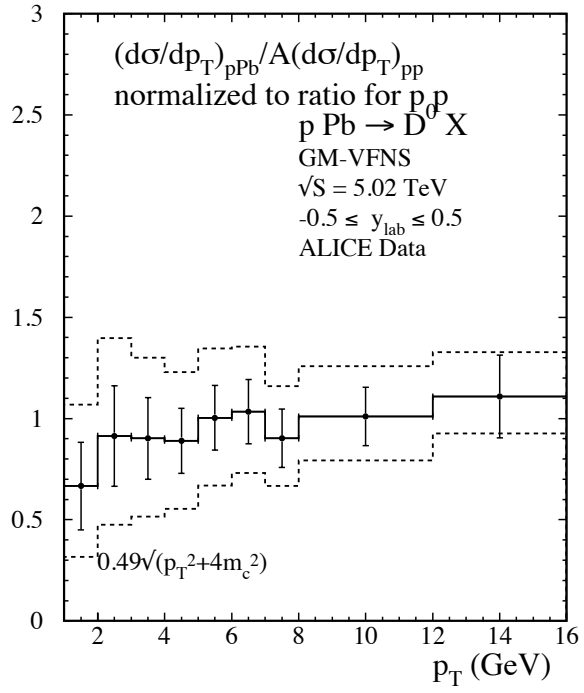

Figure 6: The ratio of ALICE data for D^0 production in p-Pb collisions at $\sqrt{S} = 5.02$ TeV over theory, normalized to the D^0 data in p-p collisions. The error bars represent the uncertainty of the p-Pb measurement.

Ref. [26] the cross sections for p-p collisions have been deduced from the measured cross sections at $\sqrt{S} = 7$ TeV by extrapolation to $\sqrt{S} = 5.02$ TeV. It would be premature to interpret the observed small deviations of the nuclear modification factors from one as a sign of initial-state interaction effects as long as we see similar deviations for p-p collisions as shown in Fig. 1, right panel. It has been shown in Ref. [26] that theoretical expectations for deviations of $R_{\rm pPb}$ from one for several models existing in the literature are rather small at large p_T, and only at very small p_T they are large enough to be compatible with the ALICE data.

3 B meson production in p-Pb collisions

Up to now, cross section data of $d\sigma/dp_T$ for B-meson production (B^+, B^0 and B_s^0) in p-Pb collisions at $\sqrt{S} = 5.02$ TeV are available only for larger p_T values above 10 GeV [30], in the range $10 < p_T < 60$ GeV. In Ref. [30] data have been compared with A times the FONLL prediction for p-p collisions [29]. At $\sqrt{S} = 7$ TeV the LHCb collaboration has measured the p-p cross section $d\sigma/dp_T$ down to $p_T = 0$ for $B^+ + \bar{B}^-$, $B^0 + \bar{B}^0$ and $B_s^0 + \bar{B}_s^0$ production in the forward region $2 \leq y \leq 4.5$ [13, 36]. These data have been compared with our GM-VFNS predictions using the *modified* scale $0.5\sqrt{m_b^2 + p_T^2}$. The comparison between the LHCb data and our predictions showed reasonably good agreement for all three B meson species [18]. In this reference we compared the GM-VFNS predictions also for B^+-meson production measured by the ATLAS collaboration [12] where data extend into the very large p_T-range, $9 < p_T < 120$ GeV, for various rapidity intervals in the range $0 < |y| < 2.25$. In this comparison we found agreement between data and theory except for the lowest p_T bin, 9-13 GeV, where the data are slightly overestimated.

In the following we show the results for $Ad\sigma/dp_T$ at $\sqrt{S} = 5.02$ TeV in the rapidity interval $|y| < 2.4$, again obtained from the p-p cross section $d\sigma/dp_T$ by multiplication with the mass number A. We have done these calculations for the *original* scale choice $\mu_o = \sqrt{m_b^2 + p_T^2}$; for the *modified* choice we decided to choose $\mu_m = 0.5\sqrt{m_b^2 + p_T^2} = 0.5\mu_o$ in order to allow for a direct comparison with the previous work [18][1]. m_b is the bottom quark mass, $m_b = 4.5$ GeV. The FF for $b \to B$ was taken from [5] for all three B meson states. Cross sections for the different B meson species differ only by their respective constant fragmentation fractions. Our results are compared to the CMS data for p-Pb collisions [30] and are shown for B^+, B^0 and B_s^0 production, respectively, in the left panels of Figs. 7, 8, and 9 for $\mu = \mu_o$ and in the right panels of these figures for $\mu = \mu_m$. As to be expected the results for the *original* scale choice μ_o lie slightly higher than for the *modified* scale choice μ_m, but the difference is decreasing towards larger p_T. For all cases data and theory agrees within theoretical and experimental errors.

[1] The value of $\mu_{I,F}$ at $p_T = 0$ is not very relevant here since we will compare with data at large p_T. With $\mu_{I,F} = 0.5\sqrt{4m_b^2 + p_T^2}$ the cross section would increase by only 12 % in the first p_T-bin (10 GeV $\leq p_T \leq$ 15 GeV) and by less than 2 % at higher p_T.

The comparison between the experimental cross section $d\sigma/dp_T$ for p-Pb scattering and the theoretical cross sections $Ad\sigma/dp_T$ becomes more clear when presented in terms of the nuclear modification factors $R_{\rm pPb} = (d\sigma/dp_T)_{\rm pPb}/A(d\sigma/dp_T)_{\rm pp}$. We show these ratios for all three B meson species and for both scale choices, μ_o and μ_m, in Figs. 10, 11, and 12 (left and right panels). We notice that with the *modified* scale choice, the ratio $R_{\rm pPb}$ agrees with one within experimental errors, even without taking into account the theory uncertainty due to scale variations given by the dashed lines in Figs. 10-12. For the *modified* scale choice our results agree also rather well with those presented in [30] where the p-p cross section used to obtain $R_{\rm pPb}$ was calculated in the FONLL approach [29].

In view of our findings for the scale setting $\mu = \mu_m$ it would be necessary to reduce experimental errors by at least a factor of two before one could claim that deviations of $R_{\rm pPB}$ from one have been observed and that nuclear initial-state interaction effects are present. For the *original* scale choice $\mu = \mu_o$ such deviations seem to occur already within present errors in some of the p_T bins as seen in Figs. 10, 11, and 12 (left panels). It seems obvious to us that also theory uncertainties will have to be reduced before a conclusive interpretation of the data will be possible. This will require the calculation of higher-oder corrections which are exptected to reduce the uncertainties due to the choice of renormalization and factorization scales.

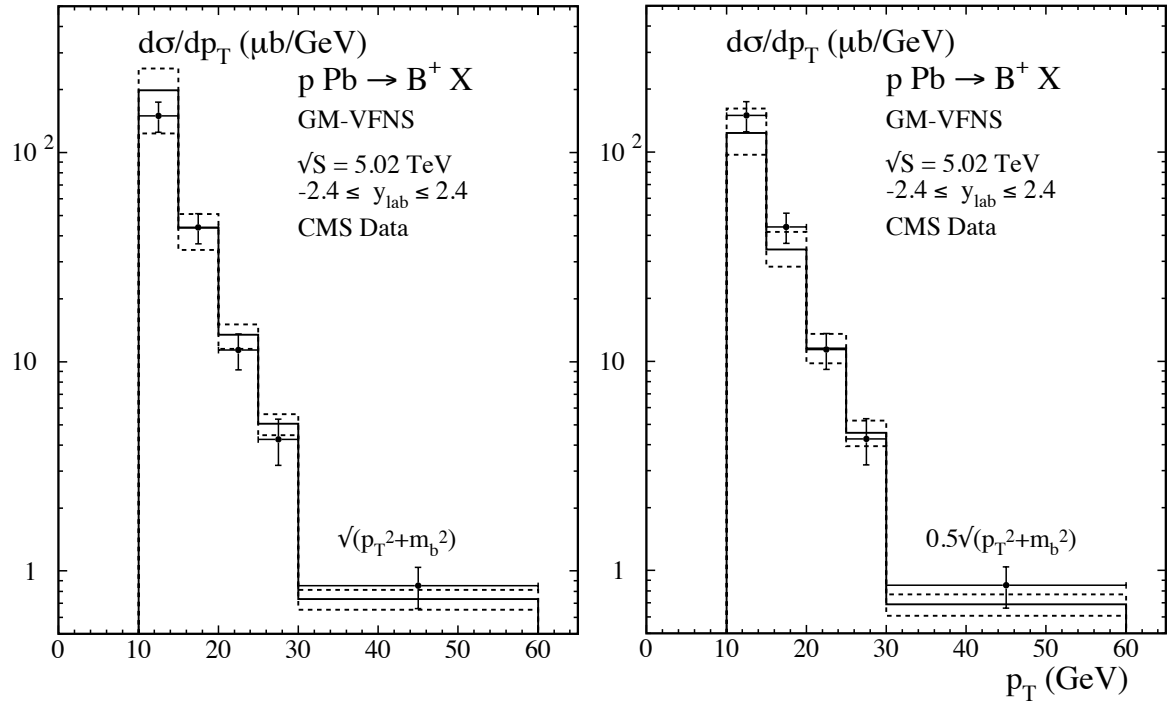

Figure 7: Differential cross section $Ad\sigma/dp_T$ as a function of the transverse momentum p_T for the inclusive production of B^+ mesons calculated in the GM-VFNS at $\sqrt{S} = 5.02$ TeV and $|y| < 2.4$ with the *original* scale choice $\mu_R = \mu_I = \mu_F = m_T$ (left panel) and with the *modified* scale choice $\mu_R = \mu_I = \mu_F = 0.5m_T$ (right panel) compared to CMS data [30].

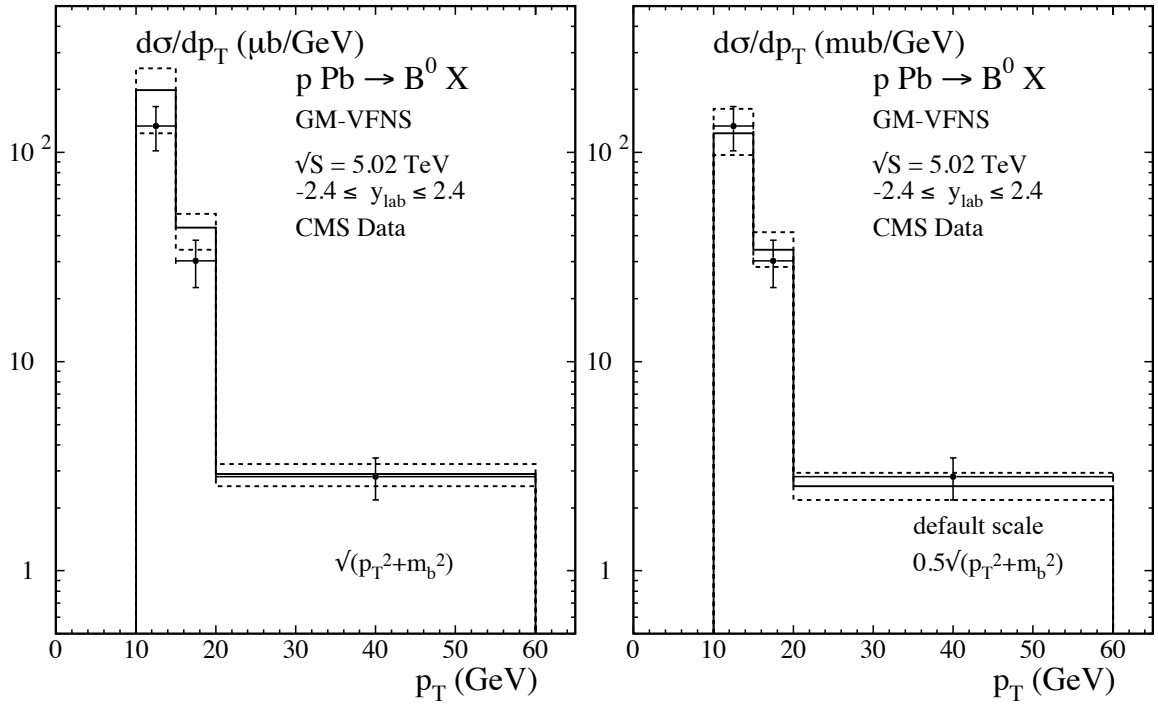

Figure 8: Differential cross section $Ad\sigma/dp_T$ as a function of the transverse momentum p_T for the inclusive production of B^0 mesons calculated in the GM-VFNS at $\sqrt{S} = 5.02$ TeV and $|y| < 2.4$ with the *original* scale choice $\mu_R = \mu_I = \mu_F = m_T$ (left panel) and with the *modified* scale choice $\mu_R = \mu_I = \mu_F = 0.5m_T$ (right panel) compared to CMS data [30].

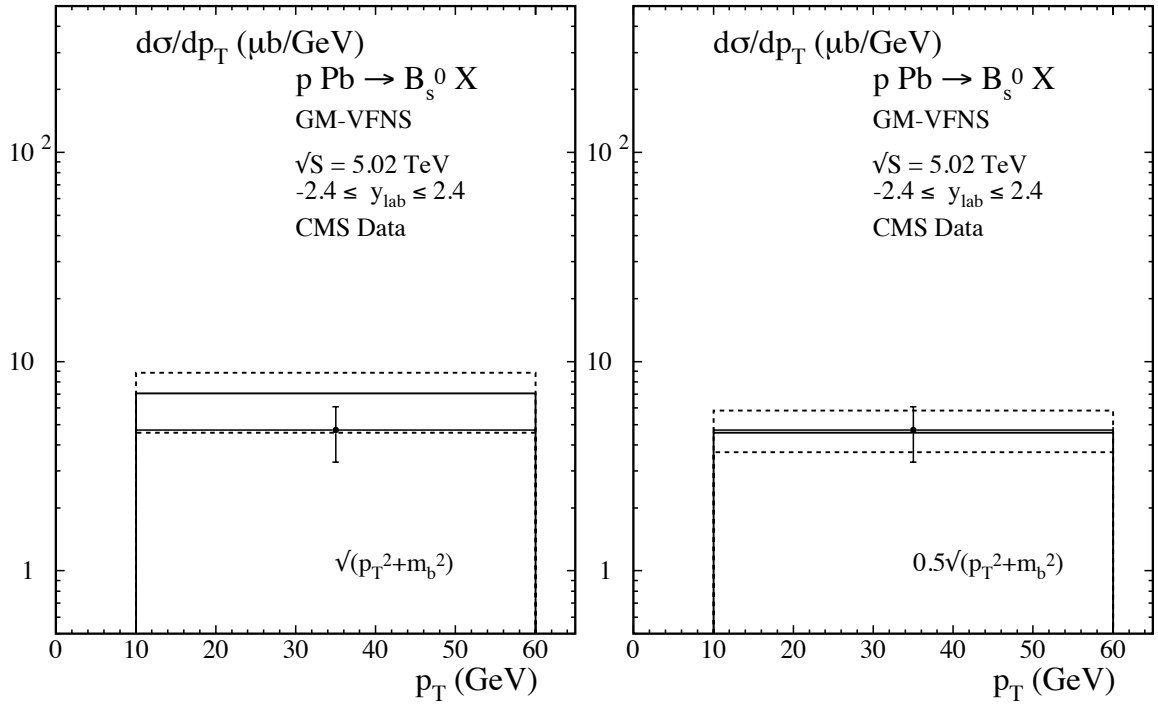

Figure 9: Differential cross section $Ad\sigma/dp_T$ as a function of the transverse momentum p_T for the inclusive production of B_s^0 mesons calculated in the GM-VFNS at $\sqrt{S} = 5.02$ TeV and $|y| < 2.4$ with the *original* scale choice $\mu_R = \mu_I = \mu_F = m_T$ (left panel) and with the *modified* scale choice $\mu_R = \mu_I = \mu_F = 0.5m_T$ (right panel) compared to CMS data [30].

4 Conclusions

We have studied D and B meson production in p-Pb collisions at NLO in the GM-VFNS and find good agreement with experimental data obtained by the LHC collaborations ALICE and CMS. Our main results are shown in the right panels of Figs. 2 - 5 for D-meson production and in Figs. 10 - 12 for B-meson production. For charmed meson production, the ratios of data over theory predictions at $p_T > 6$ GeV are compatible with one within uncertainties and deviations are not larger than 40%. At small transverse momenta, $p_T < 6$ GeV, the ratios increase to values of about 1.5 and larger. Uncertainties from both experiment and theory are, however, large. It is therefore doubtful whether this deviation can be interpreted as due to initial-state interaction effects, in particular since deviations of the same size and with a similar p_T-dependence are also present for p-p collisions. Higher precision of the measurements as well as of theory predictions is needed in order to draw firm conclusions. It will be interesting to include forthcoming more precise data in our analysis, as for example Ref. [37] which became available after completion of this work, but data are not yet publicly available.

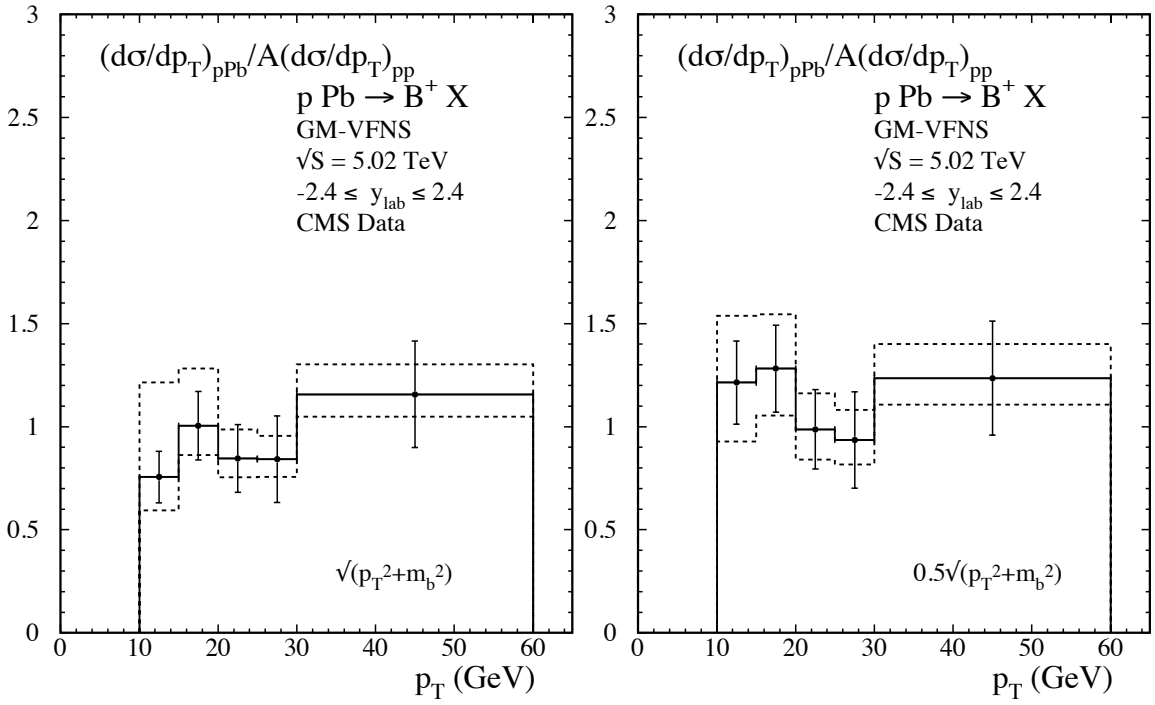

Figure 10: Ratio of the measured CMS cross section $d\sigma/dp_T$ to the GM-VFNS cross section shown in Fig. 7 for the *original* scale choice (left panel) and for the *modified* scale choice (right panel) for inclusive B^+ production.

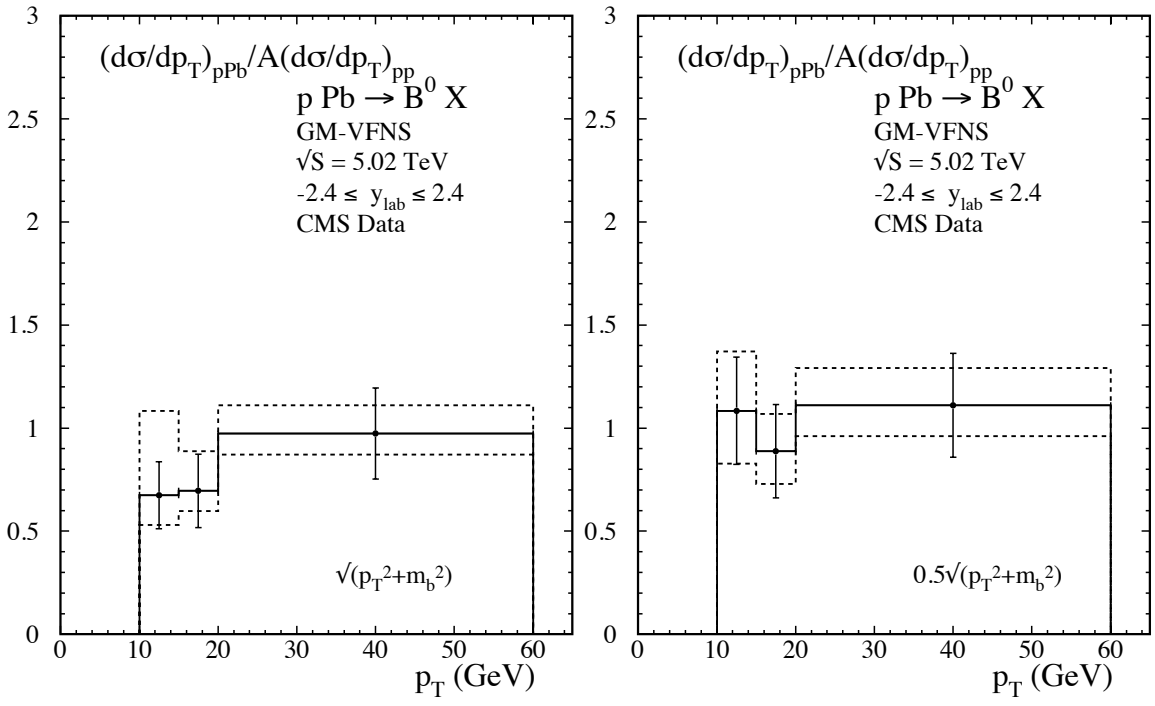

Figure 11: Ratio of the measured CMS cross section $d\sigma/dp_T$ to the GM-VFNS cross section shown in Fig. 8 for the *original* scale choice (left panel) and for the *modified* scale choice (right panel) for inclusive B^0 production.

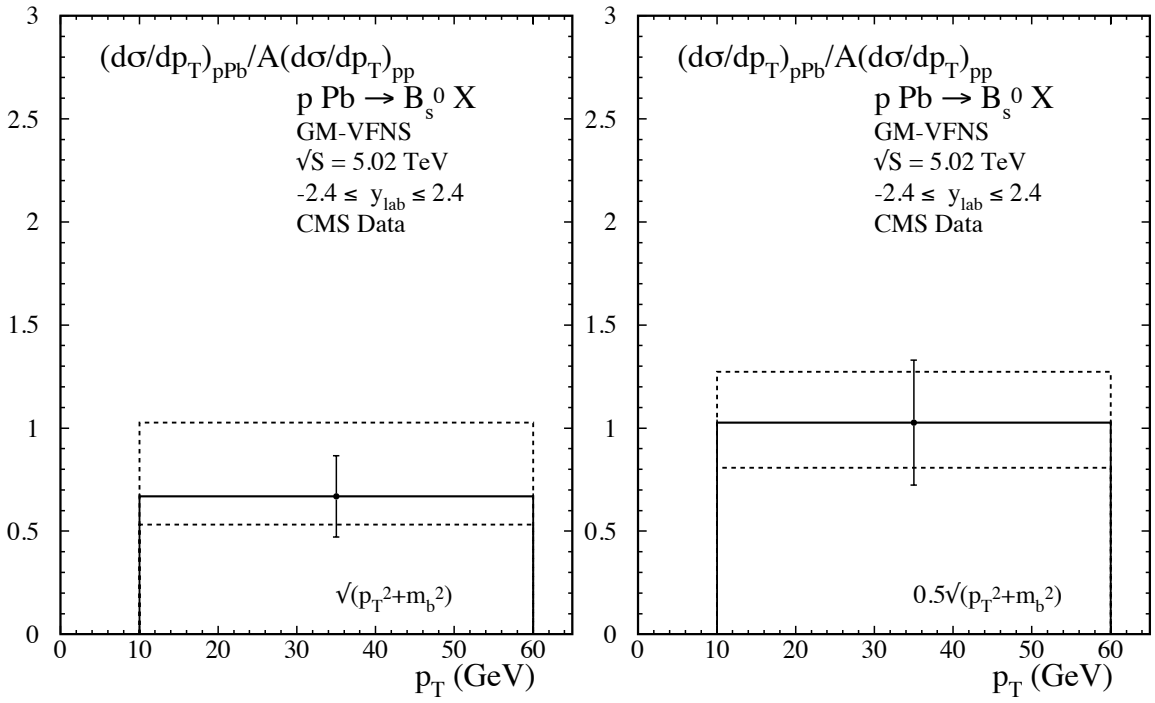

Figure 12: Ratio of the measured CMS cross section $d\sigma/dp_T$ to the GM-VFNS cross section shown in Fig. 9 for the *original* scale choice (left panel) and for the *modified* scale choice (right panel) for inclusive B_s^0 production.

References

[1] M. Cacciari, M. Greco and P. Nason, JHEP **9805** (1998) 007 [hep-ph/9803400].

[2] M. Cacciari and P. Nason, JHEP **0309** (2003) 006 [hep-ph/0306212].

[3] B. A. Kniehl, G. Kramer, I. Schienbein and H. Spiesberger, Phys. Rev. D **71** (2005) 014018 [hep-ph/0410289].

[4] B. A. Kniehl, G. Kramer, I. Schienbein and H. Spiesberger, Eur. Phys. J. C **41** (2005) 199 [hep-ph/0502194].

[5] B. A. Kniehl, G. Kramer, I. Schienbein and H. Spiesberger, Phys. Rev. D **77** (2008) 014011 [arXiv:0705.4392 [hep-ph]].

[6] D. Acosta *et al.* [CDF Collaboration], Phys. Rev. D **71** (2005) 032001 [hep-ex/0412071].

[7] A. Abulencia *et al.* [CDF Collaboration], Phys. Rev. D **75** (2007) 012010 [hep-ex/0612015].

[8] B. A. Kniehl, G. Kramer, I. Schienbein and H. Spiesberger, Phys. Rev. D **84** (2011) 094026 [arXiv:1109.2472 [hep-ph]].

[9] V. Khachatryan *et al.* [CMS Collaboration], Phys. Rev. Lett. **106** (2011) 112001 [arXiv:1101.0131 [hep-ex]].

[10] S. Chatrchyan *et al.* [CMS Collaboration], Phys. Rev. Lett. **106** (2011) 252001 [arXiv:1104.2892 [hep-ex]].

[11] S. Chatrchyan *et al.* [CMS Collaboration], Phys. Rev. D **84** (2011) 052008 [arXiv:1106.4048 [hep-ex]].

[12] G. Aad *et al.* [ATLAS Collaboration], JHEP **1310** (2013) 042 [arXiv:1307.0126 [hep-ex]].

[13] R. Aaij *et al.* [LHCb Collaboration], JHEP **1204** (2012) 093 [arXiv:1202.4812 [hep-ex]].

[14] D. Acosta *et al.* [CDF Collaboration], Phys. Rev. Lett. **91** (2003) 241804 [hep-ex/0307080].

[15] G. Aad *et al.* [ATLAS Collaboration], Nucl. Phys. B **907** (2016) 717 [arXiv:1512.02913 [hep-ex]].

[16] B. A. Kniehl, G. Kramer, I. Schienbein and H. Spiesberger, Phys. Rev. Lett. **96** (2006) 012001 [hep-ph/0508129].

[17] B. A. Kniehl, G. Kramer, I. Schienbein and H. Spiesberger, Eur. Phys. J. C **72** (2012) 2082 [arXiv:1202.0439 [hep-ph]].

[18] B. A. Kniehl, G. Kramer, I. Schienbein and H. Spiesberger, Eur. Phys. J. C **75** (2015) 140 [arXiv:1502.01001 [hep-ph]].

[19] G. Kramer and H. Spiesberger, Phys. Lett. B **753** (2016) 542 [arXiv:1509.07154 [hep-ph]].

[20] S. O. Moch, M. Benzke, M. V. Garzelli, B. Kniehl, G. Kramer and G. Sigl, PoS LL **2016** (2016) 060.

[21] M. Benzke, M. V. Garzelli, B. A. Kniehl, G. Kramer, S. Moch and G. Sigl, to be published.

[22] R. Aaij *et al.* [LHCb Collaboration], arXiv:1610.02230 [hep-ex].

[23] R. Aaij *et al.* [LHCb Collaboration], Nucl. Phys. B **871** (2013) 1 [arXiv:1302.2864 [hep-ex]].

[24] R. Aaij *et al.* [LHCb Collaboration], JHEP **1603** (2016) 159 Erratum: [JHEP **1609** (2016) 013] [arXiv:1510.01707 [hep-ex]].

[25] B. B. Abelev *et al.* [ALICE Collaboration], Phys. Rev. Lett. **113** (2014) 232301 [arXiv:1405.3452 [nucl-ex]].

[26] J. Adam *et al.* [ALICE Collaboration], Phys. Rev. C **94** (2016) 054908 [arXiv:1605.07569 [nucl-ex]].
see also: CERN Courier Vol. 57, January/February 2017, p. 11.

[27] B. Abelev *et al.* [ALICE Collaboration], JHEP **1209** (2012) 112 [arXiv:1203.2160 [nucl-ex]].

[28] B. Abelev *et al.* [ALICE Collaboration], JHEP **1201** (2012) 128 [arXiv:1111.1553 [hep-ex]].

[29] M. Cacciari, S. Frixione, N. Houdeau, M. L. Mangano, P. Nason and G. Ridolfi, JHEP **1210** (2012) 137 [arXiv:1205.6344 [hep-ph]].

[30] V. Khachatryan *et al.* [CMS Collaboration], Phys. Rev. Lett. **116** (2016) 032301 [arXiv:1508.06678 [nucl-ex]].

[31] S. Dulat *et al.*, Phys. Rev. D **93** (2016) 033006 [arXiv:1506.07443 [hep-ph]].

[32] A. Buckley, J. Ferrando, S. Lloyd, K. Nordström, B. Page, M. Rüfenacht, M. Schönherr and G. Watt, Eur. Phys. J. C **75** (2015) 132 [arXiv:1412.7420 [hep-ph]].
`http://projects.hepforge.org/lhapdf/pdfsets`

[33] T. Kneesch, B. A. Kniehl, G. Kramer and I. Schienbein, Nucl. Phys. B **799** (2008) 34 [arXiv:0712.0481 [hep-ph]].

[34] B. A. Kniehl and G. Kramer, Phys. Rev. D **74** (2006) 037502 [hep-ph/0607306].

[35] R. Maciula and A. Szczurek, Phys. Rev. D **87** (2013) 094022 [arXiv:1301.3033 [hep-ph]].

[36] R. Aaij *et al.* [LHCb Collaboration], JHEP **1308** (2013) 117 [arXiv:1306.3663 [hep-ex]].

[37] S. Acharya *et al.* [ALICE Collaboration], arXiv:1702.00766 [hep-ex].